

Soliton acceleration by dispersive radiation: a contribution to rogue waves?

A. Demircan

Invalidenstr. 114, 10115 Berlin, Germany

Sh. Amiranashvili and C. Brée

Weierstrass Institute for Applied Analysis and Stochastics, Mohrenstraße 39, 10117 Berlin, Germany

Ch. Mahnke and F. Mitschke

Institute for Physics, University of Rostock, Universitätsplatz 3, 18055 Rostock, Germany

G. Steinmeyer

Max Born Institute for Nonlinear Optics and Short Pulse Spectroscopy,

Max-Born-Straße 2A, 12489 Berlin, Germany and

Optoelectronics Research Centre, Tampere University of Technology, 33101 Tampere, Finland

(Dated: October 26, 2021)

Rogue waves are solitary waves with extreme amplitudes, which appear to be a ubiquitous phenomenon in nonlinear wave propagation, with the requirement for a nonlinearity being their only unifying characteristics. While many mechanisms have been demonstrated to explain the appearance of rogue waves in a specific system, there is no known generic mechanism or general set of criteria shown to rule their appearance. Presupposing only the existence of a nonlinear Schrödinger-type equation together with a concave dispersion profile around a zero dispersion wavelength we demonstrate that solitons may experience acceleration and strong reshaping due to the interaction with continuum radiation, giving rise to extreme-value phenomena. The mechanism is independent of the optical Raman effect. A strong increase of the peak power is accompanied by a mild increase of the pulse energy and carrier frequency, whereas the photon number of the soliton remains practically constant. This reshaping mechanism is particularly robust and may explain the appearance of rogue waves in a large class of systems.

PACS numbers: 42.65.-k, 42.81.Dp, 47.35.Fg, 04.70.-s

The appearance of waves with extreme amplitude has been investigated in a large class of physical systems [1–8]. Their appearance is most drastically illustrated for the case of ocean waves [9–11], with waves exceeding the average wave crest by a factor three or more and causing serious damage to ocean-going ships. Recently, similar phenomena have also been reported in optics in the soliton-supporting red tail of supercontinua (SC) in fibers [8]. Substantial progress has been made in the understanding of the mechanisms behind optical rogue waves [12–15]. Currently, most explanations follow one of two alternatives. One involves soliton fission and selective Raman shifting of the largest solitons to the long-wavelength side of the spectrum [13, 14]. The other builds on the dynamics of Akhmediev breathers [15] and inelastic collisions between solitons or breathers. While these explanations concentrate either on soliton fission or fusion processes, we demonstrate in the following that a similar mechanism may exist between solitons and continuum radiation in the normal dispersion range. We will refer to the latter as dispersive wave (DW). Suitable conditions provided, this DW can strongly modify a soliton through cross phase modulation (XPM). Strong reshaping, in particular temporal compression, of the soliton is accompanied by a mild increase of its energy and carrier frequency, while the photon number of the soliton re-

mains practically constant. Decrease of the center wavelength gives rise to acceleration of the soliton by virtue of dispersion. The soliton peak power grows surprisingly and may more than double in only a few centimeters of propagation.

In the following, we consider the rogue wave formation in the SC generation in a single-mode photonic crystal fiber with one zero dispersion wavelength (ZDW), which is similar to the fiber used in [8, 16]. In the following, we restrict our analysis to the minimum set of optical effects necessary for the formation of rogue waves. These effects include dispersion and the Kerr nonlinearity, yet exclude Raman scattering, cf. [16]. In the fiber geometry, the optical field is characterized by a single real valued component $E(z, t)$ whereas dependencies perpendicular to the propagation coordinate z are integrated out. We choose a suitable time period T , introduce frequencies $\omega \in 2\pi\mathbb{Z}/T$, denote spectral field components by $E_\omega(z)$, and following [17] define a complex valued $\mathcal{E}(z, t)$ such that $\mathcal{E}_\omega(z) = E_\omega(z) - i\partial_z E_\omega(z)/|\beta(\omega)|$. Note that $E = \text{Re}[\mathcal{E}]$, the propagation equation for $\mathcal{E}(z, t)$ reads

$$i\partial_z \mathcal{E}_\omega + |\beta(\omega)|\mathcal{E}_\omega + \frac{3\omega^2 \chi^{(3)}}{8c^2 |\beta(\omega)|} (|\mathcal{E}|^2 \mathcal{E})_\omega = 0. \quad (1)$$

Parameters c , $\chi^{(3)}$, and $\beta(\omega)$ are the speed of light, the third-order nonlinear susceptibility, and the propagation

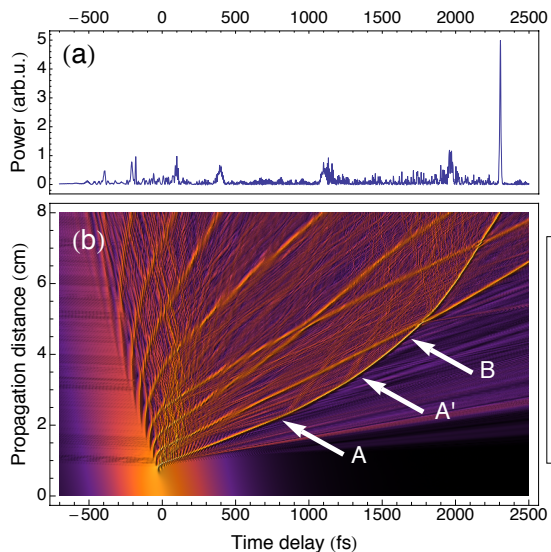


FIG. 1: Temporal evolution of a higher-order soliton injected close to the ZDW into the fiber along z for a typical SC generation process. Note that the calculation does not involve the Raman effect. (a) Final state with a rogue wave exceeding the average wave crest by more than a factor of three. (b) Propagation dynamics of the solitons and non-solitonic radiation, generated by the fission process.

constant respectively. Equation (1) is subject to the conservation laws

$$I_1 = \sum_{\omega} \frac{n(\omega)}{\omega} |\mathcal{E}_{\omega}|^2, \quad I_2 = \sum_{\omega} n(\omega) |\mathcal{E}_{\omega}|^2 \quad (2)$$

where $n(\omega)$ is refractive index and $I_{1,2}$ are finite and proportional to the time-averaged photon flux and power respectively [17]. For unidirectional propagation $\mathcal{E}(z, t)$ is identical to analytic signal $\mathcal{E}(z, t) = 2 \sum_{\omega > 0} E_{\omega}(z) e^{-i\omega t}$ and moreover only the positive-frequency part of $|\mathcal{E}|^2 \mathcal{E}$ contributes to Eq. (1). The fiber propagation constant may be obtained by numerical integration of the group delay $\beta_1(\omega) = \beta'(\omega)$ and then approximated following [18]. If the slow envelope description with respect to a carrier frequency ω_0 applies, Eq. (1) reduces to the standard nonlinear Schrödinger equation [19] with the nonlinearity parameter $\gamma = (3\omega_0 \chi^{(3)}) / [4\epsilon_0 c^2 n^2(\omega_0) A_{\text{eff}}]$, where A_{eff} is the effective fiber area. Beyond the standard treatment with an envelope approximation, our approach correctly models nonlinear processes between spectrally disparate waves, i.e., four-wave mixing processes and XPM between solitons and DWs, and between individual solitons. These nonlinear processes have been previously found important for explaining rogue waves in gravity matter waves [10].

We launch a hyperbolic secant pulse (center wavelength 897 nm, full width at half maximum FWHM = 265 fs), corresponding to a higher-order soliton with soliton number $N \approx 28$ in the anomalous dispersion regime of

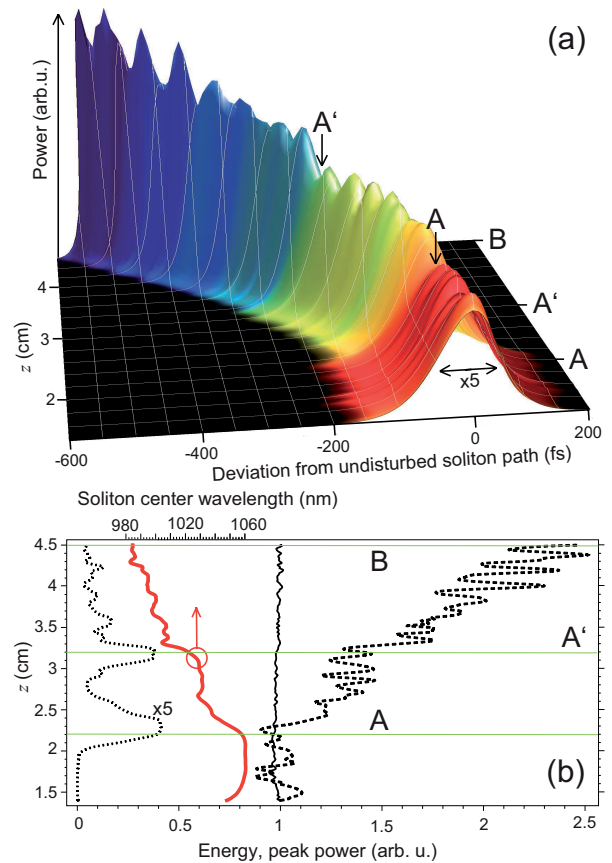


FIG. 2: (a) Visualization of the soliton propagating from A to B in Fig. 1. Temporal delays are shown relative to the unperturbed propagation of the soliton at $z = 1.5\text{--}2$ cm. For clarity, the width of the soliton has been stretched by a factor 5. Color coding visualizes $\lambda_0(z)$, which changes from 1060 to 985 nm (red and blue, respectively). (b) Development of soliton parameters $\lambda_0(z)$ (thick red line), pulse energy $\propto I_2$ (solid black line), and peak power $P_0(z)$ (dashed line). Energy content of the dispersive wave within $\pm 1.5\tau$ interval around $t_*(z)$ is shown as a dotted line.

the fiber close to the ZDW = 842 nm. For a nonlinear fiber with $\gamma = 0.1 \text{ W}^{-1} \text{ m}^{-1}$ this corresponds to a peak power of 19 kW, so that soliton fission is favored [20]. These conditions ensure the formation of a SC with the increase of the initial spectral width by one to two orders of magnitude [21]. Figure 1 shows the typical SC evolution in the temporal domain. With the rather moderate powers in this example, the effect of the modulational instability can only be observed in the initial ≈ 0.5 cm propagation length before pulses reach the sub-100 fs regime [22]. The fundamental solitons produced in the fission process exhibit durations between 10 and 20 fs with different peak powers, appearing as pronounced lines which clearly stand out from the background. The fission process also generates DWs in the normal dispersion regime [21]. The further away from the ZDW solitons are being generated, the slower they will propagate

[22], accumulating delay (Fig. 1). As we deliberately excluded Raman scattering in our analysis, we might expect that the group velocity of solitons is constant except in places where isolated soliton-soliton scattering processes occur. Indeed, inspection of Fig. 1 reveals several such characteristic crossings of soliton trajectories in the t - z plane. However, it also reveals that the trajectory of the strongest soliton does not appear to be ruled by rare isolated scattering events (AB, Fig. 1). The parabolic trajectory of this soliton is witness of its constant acceleration.

To elucidate the physical mechanisms behind this peculiar acceleration, we numerically isolated the soliton, separated it from accompanying continuum radiation, and fitted the model function $f(t) = P_0 \text{sech}^2[(t - t_*)/t_0]$ to its intensity envelope (Fig. 2, FWHM $\tau = 1.76t_0$). Compared to the steady propagation at $z < 2.2$ cm, Fig. 2(a) confirms a deviation of $t_*(z)$ from the initial linear trajectory by -600 fs at point B ($z = 4.5$ cm). This temporal shift is accompanied by a 4% change of pulse energy $\propto I_2$ and by a more than twofold increase of peak power $P_0(z)$, [solid and dashed curves in Fig. 2(b), respectively]. Pulse duration scales accordingly from an initial 20 fs (FWHM) to sub-10 fs at B. Furthermore, a Fourier analysis indicates that the center wavelength $\lambda_0(z)$ of the soliton shifts from 1060 to 985 nm within the 2.3 cm propagation from A to B, reflecting the according energy transfer.

Rogue waves, subject to non-Gaussian statistics, have been shown to appear in the fiber SC generation both with and without Raman frequency shift in [16]. The rogue event regarded as an emerging single “champion” soliton was linked to multiple collisions between optical solitons. As in our case there is no other soliton in reach from A to B, this parameter change can only be explained by nonlinear continuum-soliton interaction. Namely, for each soliton velocity there is a spectral slice of dispersive non-solitonic radiation which propagates at nearly identical group velocity. Group-velocity matching significantly increases the nonlinear interaction length between continuum and soliton [21, 23] and may lead to the reshaping of the latter [26]. Comparing to the energy of the DW that is in temporal overlap with the soliton [dotted line in Fig. 2(b)], it is striking that changes of each of the soliton parameters $t_*(z)$, $\lambda_0(z)$, and $P_0(z)$ are strongly correlated with the strength of the DW, see positions A and A' marked in Fig. 2. It appears still surprising that a DW with less than 10% of the soliton amplitude can affect its properties so strongly.

For further investigation of this scenario, we numerically isolated the primary soliton and selected segments of the DW in Fig. 1(a) right at the onset of the trajectory curvature, allowing for a deterministic interpretation of the acceleration process of the soliton uncoupled from the SC generation process. To this end, we inject into the fiber a fundamental soliton at $\lambda_s = 1030$ nm of 26.6 fs

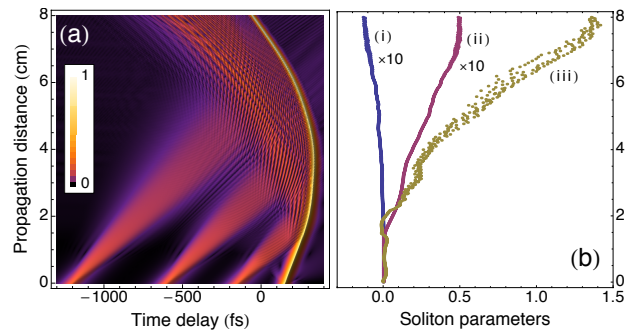


FIG. 3: (a) Time domain evolution along the fiber representing the isolated trajectory of a fundamental soliton. Acceleration results from a cascaded scattering with three DWs. (b) Relative change of soliton parameters: (i) photon number (see Eq. (2) and [17]), (ii) energy, (iii) peak power. The deviation of a parameter ζ is defined as $[\zeta(t) - \zeta(0)]/\zeta(0)$. For clarity, deviations (i) and (ii) have been stretched by a factor 10.

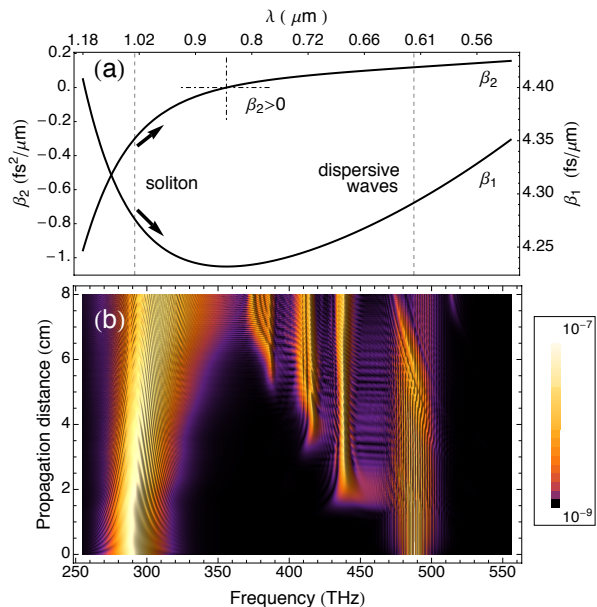


FIG. 4: (a) Exemplary concave group delay $\beta_1 = \beta'(\omega)$ and related group-velocity dispersion $\beta_2 = \beta''(\omega)$, with the extracted wavelengths for the fundamental soliton at $\lambda_s = 1030$ nm and a dispersive pulse at $\lambda_d = 614$ nm (dashed line). Arrows indicate the induced change of β_2 and β_1 for the soliton. (b) Spectral evolution along the fiber representing a cascaded scattering with three DWs from a soliton.

FWHM duration together with slightly slower propagating 53.2 fs time segments of DWs near the velocity-matched wavelength of $\lambda_d = 614$ nm.

Figure 3(a) demonstrates an example for a continuum-soliton scattering process with three DWs in a suitably chosen reference frame. Each collision leads to a stepwise acceleration of the soliton, clearly confirming the transfer of energy and the concomitant gradual increase in peak power [Fig. 3(b)] as previously seen in Fig. 2. As all ob-

scuring continuum components have been eliminated, the role of the dispersive radiation can now be seen in much greater clarity. The DWs initially propagate at slightly lower group velocity than the trailing soliton so that they eventually collide. In this collision, the soliton can never pass the DW as would be expected in a purely linear-optical encounter. Instead, XPM between DW and soliton causes a frequency shift towards the ZDW (842 nm), decreasing the center wavelength of the soliton and shifting the DW toward longer wavelength. Comparing to the underlying dispersion profile [Fig. 4(a)], both these shifts lead to an acceleration for the respective type of radiation, as is clearly confirmed by the trajectory curvatures in Fig. 3(a).

Under similar conditions, the impenetrability of the soliton trajectory was referred to as an optical event horizon for the DW [25, 26]. Its origin lies in a nonlinearly induced increase of the group velocity caused by the leading edge of the soliton. The only way for the DW to escape from the event horizon is a shift towards the ZDW, i.e., both types of radiation therefore experience a strongly enhanced effective XPM. These processes are completely elastic, causing a mutual shift of optical frequencies but never transferring photons from the normal dispersion regime into the soliton regime or vice versa. With the photon number of the soliton practically conserved, the soliton blue shift accordingly causes a mild increase of its energy [Fig. 3(b)]. The shifted soliton also experiences a considerably smaller β_2 [Fig. 4(a,b)]. Now consider that the energy of a fundamental soliton can be expressed through P_0 and β_2 as $E = 2\sqrt{P_0|\beta_2|/\gamma}$. Obviously, the decrease of β_2 cannot be compensated by a reduction of E because E also grows. As γ does not vary appreciably, consequently, P_0 is forced to grow massively. This clearly explains our observations. We repeated these simulations with several segments of continuum to prove that even higher soliton peak powers can be achieved with segments of the continuum containing more energy.

The nature of the newly observed continuum-soliton scattering processes is markedly different from soliton-soliton scattering. As continuum radiation quickly disperses, there will always be temporal slices of the DW that effectively copropagate with a given soliton, making mutual extended interaction much more likely than the appearance of soliton-soliton processes. We therefore suggest that this mechanism contributes to the dramatic amplitude increases seen in experimental work [8].

The mechanism proposed here does not presuppose any special nonlinear effects that are unique to optical systems. In comparison to previously discussed mechanisms of rogue wave formation, our approach essentially only presupposes a nonlinear Schrödinger type scenario, with a reactive nonlinearity and a concave dispersion profile, the latter enabling copropagation of radiation with opposite signs of dispersion with equal group velocity. These conditions are met in a variety of systems, e.g., for

gravity-capillary waves [27]. Our explanation is therefore immediately applicable to a much wider class of physical systems. Consequently, we believe that the previously disregarded scattering of DWs off solitons opens a new perspective on the fascinating appearance of extreme-value wave phenomena.

The following support is gratefully acknowledged: Sh. A. by the DFG Research Center MATHEON (project D 14), C. M. and F. M. by DFG, and G. S. by the Academy of Finland (project grant 128844).

-
- [1] K. Dysthe, H. E. Krogstad, and P. Müller, *Annu. Rev. Fluid Mech.* **40**, 287 (2008).
 - [2] A. N. Ganshin *et al.*, *Phys. Rev. Lett.* **101**, 065303 (2008).
 - [3] Yu. V. Bludov, V. V. Konotop, and N. Akhmediev, *Phys. Rev. A* **80**, 033610 (2009).
 - [4] M. S. Ruderman, *Eur. Phys. J. Special Topics* **185**, 57 (2010).
 - [5] L. Stenflo and M. Marklund, *J. Plasma Phys.* **76**, 293 (2010).
 - [6] J. Kasparian *et al.*, *Opt. Express* **17**, 12070 (2009).
 - [7] D. Majus *et al.*, *Phys. Rev. A* **83**, 025802 (2011).
 - [8] D. R. Solli *et al.*, *Nature* **450**, 1054 (2007).
 - [9] C. Kharif and E. Pelinovsky, *Eur. J. Mech.* **22**, 603 (2003).
 - [10] P. A. E. M. Janssen, *J. Phys. Oceanography* **33**, 863 (2010).
 - [11] M. Onorato *et al.*, *Phys. Rev. Lett.* **86**, 5831 (2001).
 - [12] A. Mussot *et al.*, *Opt. Exp.* **17**, 1502 (2009); M. Taki *et al.*, *Phys. Lett. A* **374**, 691 (2010).
 - [13] D. R. Solli, C. Ropers, and B. Jalali, *Phys. Rev. Lett.* **101**, 233902 (2008).
 - [14] J. M. Dudley, G. Genty, B. J. Eggleton, *Opt. Exp.* **16**, 3644 (2008); M. Ekintalo, G. Genty, and J. M. Dudley, *Opt. Lett.* **35**, 658 (2010); G. Genty, J. M. Dudley, B. J. Eggleton, *Appl. Phys. B* **94**, 187 (2009).
 - [15] N. Akhmediev, J. M. Soto-Crespo, and A. Ankiewicz, *Phys. Rev. A* **80**, 043818 (2009); N. Akhmediev, A. Ankiewicz, and M. Taki, *Phys. Lett. A* **373**, 675 (2009); B. Kibler *et al.*, *Nature Physics* **6**, 790 (2010).
 - [16] G. Genty *et al.*, *Phys. Lett. A* **374** 989 (2010).
 - [17] Sh. Amiranashvili, A. Demircan, *Phys. Rev. A* **82**, 013812 (2010).
 - [18] Sh. Amiranashvili, U. Bandelow, A. Mielke, *Opt. Commun.* **283**, 480 (2009).
 - [19] G. Agrawal, *Nonlinear Fiber Optics* (Academic Press, San Diego, 2001).
 - [20] J. Herrmann *et al.*, *Phys. Rev. Lett.* **88**, 173901 (2002).
 - [21] J. M. Dudley, G. Genty, S. Coen, *Rev. Mod. Phys.* **78**, 1135 (2006).
 - [22] A. Demircan and U. Bandelow, *Appl. Phys. B* **86**, 31 (2007); *Opt. Comm.* **244**, 181 (2005).
 - [23] R. Driben, F. Mitschke, and N. Zhavoronkov, *Opt. Exp.* **18**, 25993 (2010).
 - [24] T. G. Philbin *et al.*, *Science* **319**, 1367 (2008).
 - [25] F. Belgiorno *et al.*, *Phys. Rev. Lett.* **105**, 203901 (2010).
 - [26] A. Demircan, Sh. Amiranashvili, G. Steinmeyer, *Phys. Rev. Lett.* **106**, 163901(2011).

- [27] H. Lamb, *Hydrodynamics* (6th ed.), Cambridge University Press (1994).